



Cite this: *Dalton Trans.*, 2015, **44**, 14854

Photoswitching a molecular catalyst to regulate CO₂ hydrogenation†

Nilusha Priyadarshani, Bojana Ginovska, J. Timothy Bays, John C. Linehan* and Wendy J. Shaw*

Inspired by nature's ability to regulate catalysis using physiological stimuli, azobenzene was incorporated into Rh(bis)diphosphine CO₂ hydrogenation catalysts to photoinitiate structural changes to modulate the resulting catalytic activity. The rhodium bound diphosphine ligands (P(Ph₂)-CH₂-N(R)-CH₂-P(Ph₂)) contain the terminal amine of a non-natural amino acid, with the R-group being either β-alanine (β-Ala) or γ-aminobutyric acid (GABA). For both β-Ala and GABA containing complexes, the carboxylic acids of the amino acids were coupled to the amines of diaminoazobenzene, creating a complex consisting of a rhodium bound to a photo-responsive tetradentate ligand. The photo-induced *cis*-*trans* isomerization of the azobenzene-containing complexes imposes structural changes on these complexes, as evidenced by NMR studies. We found that the CO₂ hydrogenation activity for the β-Ala bound rhodium complex is 40% faster at 27 °C with the light on, *i.e.* azobenzene in the *cis*-conformation (TOF = 16 s⁻¹) than when the complex was in the dark and the azobenzene in the *trans*-conformation (TOF = 11 s⁻¹). In contrast the γ-aminobutyric acid containing rhodium complex has the same rate (TOF ~17 s⁻¹) with the azobenzene in either the *cis* or the *trans*-conformation at 27 °C. The corresponding (bis)diphosphine complexes without the attached azobenzene were also prepared, characterized, and catalytically tested for comparison, and have TOF's of 30 s⁻¹. Computational studies were undertaken to evaluate if the difference in rate between the *cis*- and *trans*-azobenzene isomers for the β-Ala bound rhodium complex were due to structural differences. These computational investigations revealed major structural changes between all *cis*- and *trans*-azobenzene structures, but only minor structural changes that would be unique to the β-Ala bound rhodium complex. We postulate that the different rates between the *cis*- and *trans*-azobenzene β-Ala bound containing rhodium complexes are due to subtle changes in the bite angle arising from steric strain due to the azobenzene-containing tetradentate ligand. This strain alters the hydricity of the subsequent rhodium hydride and consequently the rate.

Received 2nd May 2015,
Accepted 22nd July 2015

DOI: 10.1039/c5dt01649e

www.rsc.org/dalton

Introduction

Cooperation between structure and motion contributes to the impressive performance of enzymes.¹ Structural and mechanistic studies have revealed roles of dynamics in controlling substrate access,¹ synchronizing reactions,¹ changing the ligand structure,² or even changing the active site structure.³ For example, a report by Dorothee Kern *et al.* demonstrates that the structure of adenylate kinases undergoes a dramatic conformational change which closes some of the open sites, excluding bulk water from the active site, and bringing the reactant into the active site for catalysis to occur.⁴ This and

many other examples highlight the importance of controlled structural switching in enzymatic catalysis.^{1a}

Inspired by the connection between the structure, dynamics, and function of these bio-catalysts, our group is investigating the role of a structurally switchable outer coordination sphere on molecular catalysts. Implementing structural regulation into molecular catalysts is in its infancy, and many previous demonstrations of this control have relied upon changes in solubility to affect activity. For instance, Bergbreiter *et al.* designed thermally responsive smart catalysts by incorporating poly-*N*-isopropyl acrylamide (pNIPAAm) into a block copolymer which is bound to a phosphine-ligated metal complex.⁵ Due to a structural change above 35 °C, pNIPAAm becomes insoluble, allowing the catalyst to be turned off by precipitation, and the precipitated catalyst to be recovered. Attachment of molecular catalysts to polymers for the purpose of catalyst recoverability, with and without stimulus control, has been a common theme.⁶ Using a similar approach, we

Pacific Northwest National Laboratory, Richland, WA 99354, USA.

E-mail: wendy.shaw@pnnl.gov, john.linehan@pnnl.gov; Fax: 509-371-6498;

Tel: 509-375-5922, 509-375-3983

† Electronic supplementary information (ESI) available. See DOI: 10.1039/c5dt01649e

attached pNIPAAm to the well understood Rh(bis)diphosphine for hydrogenation of alkenes and demonstrated catalytic hydrogenation of 2-butenol.⁷

Maintaining solubility while switching structure/reactivity more directly mimics enzyme function and has the potential to enable a number of different ways to control catalysis. There have been a number of approaches to this, for example, altering the structure of a supramolecular complex to control steric accessibility,⁸ using redox potentials to control non-catalytic metal properties,⁹ and using protons to control oxidation potentials.¹⁰

Photolysis of appropriately modified molecular catalysts has also been used as a means of controlling reactivity with an external stimulus. While some of these complexes take advantage of inducing charge transfers or altering luminescent properties of the core catalyst,¹¹ the overwhelming majority of examples using light as a stimulus incorporate molecules such as azobenzene or stilbene, molecules which change conformation upon photolysis.¹² One of the first azobenzene-based (non-metal) photoswitchable catalysts was reported in 1981 by Ueno *et al.*¹³ In their work, azobenzene bound β -cyclodextrin was active for ester hydrolysis where substrate access to the pocket, and consequently catalytic activity, was controlled by the *cis-trans* isomerization of azobenzene. More recently, azobenzene was attached to two zinc catalysts and the resulting complex was demonstrated to have controllable reactivity for DNA cleavage, where the *cis-trans* isomerization changed the relative positioning of the zinc complexes, hindering or promoting their cooperativity.^{12c}

Our photoswitchable catalysts build upon the Rh(bis)diphosphine complexes we have developed for CO₂ hydrogenation (Fig. S1†) which contain amino acids,¹⁴ serving as attachment points for azobenzene. The development of this core complex serves as a foundation upon which we can investigate a struc-

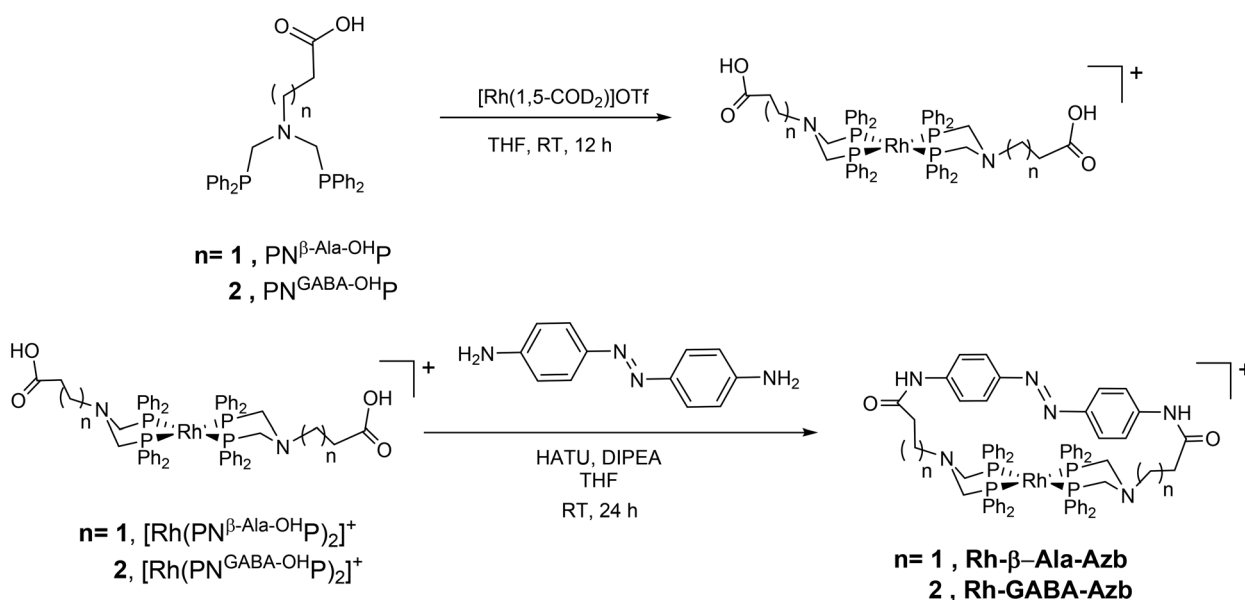
turally controllable outer coordination sphere. Herein, we build upon our previous work by attaching non-natural amino acids into the Rh(bis)diphosphine complex. To this we couple a single azobenzene across the complex to both amino acids, creating a photo-responsive tetradentate ligand.¹⁵ Our experimental results suggest that when the azobenzene ligand introduces steric strain, the *cis-trans* isomerization of azobenzene regulates catalytic activity.

Results

Synthesis and characterization of photo-responsive azobenzene Rh(bis)diphosphine complexes

Two methodologies were attempted to synthesize the desired metal complexes. Pre-forming the intact tetra-dentate phosphine ligand followed by attachment to the metal core was attempted first. While ligand synthesis and attachment of the azobenzene bridge to the two bidentate phosphine ligands was accomplished, subsequent coordination of the rhodium metal resulted in multiple metal complexes as evident from ³¹P NMR spectroscopy.

The second approach was to coordinate two bidentate ligands to the rhodium metal center and then join the ligands with an azobenzene linker. This approach resulted in the desired product. The synthesis, purification, and characterization of bidentate P(Ph)₂N^RP(Ph)₂ ligands (PN^RP) and corresponding [Rh(PN^RP)₂]⁺ complexes, where R = CH₂CH₂COOH (β -alanine or β -Ala) and R = CH₂CH₂CH₂COOH (γ -aminobutyric acid or GABA) followed a previously reported procedure,¹⁴ to result in [Rh(PN ^{β -Ala-OH}P)₂]⁺ and [Rh(PN^{GABA-OH}P)₂]⁺ in good yield (Scheme 1). These carboxylic acid functionalized [Rh(PN^RP)₂]⁺ metal complexes were bridged by chemically coupling them with one equivalent of 4,4'-diaminoazobenzene



Scheme 1 Synthetic scheme for azobenzene cross-linked Rh-R-Azb complexes.

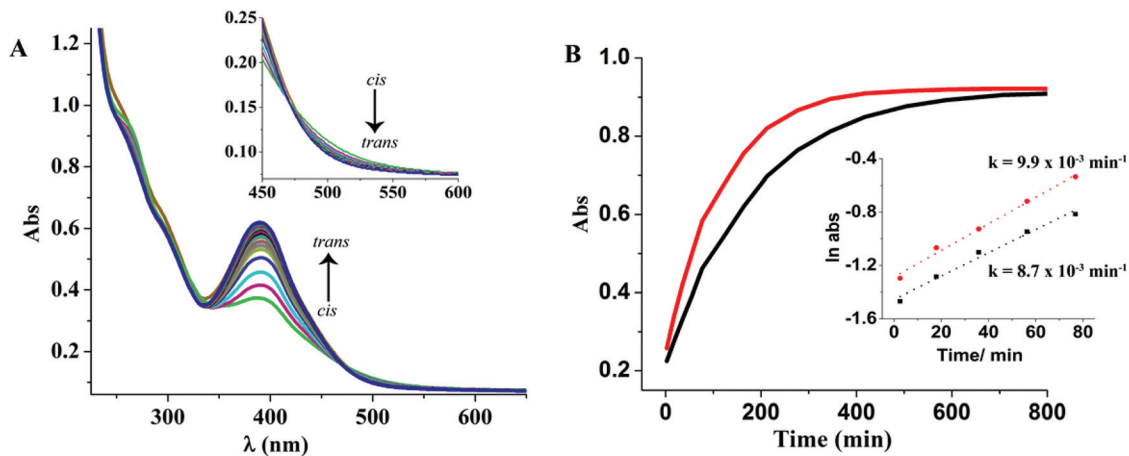


Fig. 1 (A) UV/Vis spectra of Rh- β -Ala-Azb (0.2 mM in *N*-methyl-2-pyrrolidinone (NMP)) as a function of time, tracking the *cis*-to-*trans* isomerization after irradiation with 375 nm light. Inset shows the feature at 500 nm. (B) Time profile of the *cis*-to-*trans* isomerization of Rh- β -Ala-Azb (black) and Rh-GABA-Azb (red) by monitoring the absorbance at 375 nm. Inset shows the relative rates of relaxation from *cis*-to-*trans* for both complexes, indicating that Rh- β -Ala-Azb is slower.

using 1-[bis(dimethylamino)methylene]-1*H*-1,2,3-triazolo[4,5-*b*]pyridinium 3-oxid hexafluorophosphate (HATU) as the coupling reagent (Scheme 1) in the presence of an organic base such as diisopropylethyl amine (DIPEA) to yield $[(\text{PNP})\text{Rh}(\text{PNP})\text{Azb}]^+$, annotated as (Rh- β -Ala-Azb or Rh-GABA-Azb), in fair yield. The reaction was maintained at high dilution (2.5 mM $[\text{Rh}(\text{PNR}^{\text{P}})_2]^+$). The azobenzene containing metal complexes were then obtained by partial evaporation of the reaction solvent and purified by precipitation of the complex with diethyl ether.

Both azobenzene containing complexes were characterized by ^1H and $^{31}\text{P}\{^1\text{H}\}$ NMR spectroscopy and ESI-MS, all of which are consistent with the proposed structures (Fig. S2 and S3 \dagger). The newly formed amide bond was confirmed by ^1H NMR where the amide proton (CONH) was apparent at 10.0–10.2 ppm in $\text{H}_2\text{O}/\text{THF}$ (but not $\text{D}_2\text{O}/\text{THF}$) (Fig. S2 and S3 \dagger). The absence of potential byproducts was also confirmed by mass spectroscopy, which lacked corresponding masses for complexes containing two azobenzenes, complexes with azobenzene attached at only one end, or complexes containing multiple metal units (*i.e.* polymers).

Isomerization studies of the azobenzene rhodium complexes

The UV/Vis spectrum of azobenzene shows two well separated bands in the UV/Vis region (average $\lambda_{\text{max}} \sim 375$ nm (strong) and 500 nm (weak)).¹⁶ The strong UV band arises from the $\pi \rightarrow \pi^*$ transition of the N=N bond, and the weaker absorbance band in the visible region arises from the $n \rightarrow \pi^*$ transition, with specific values being dependent upon substituents.¹⁶ Similarly, these major absorbance bands were apparent in the UV/Vis spectra of Rh- β -Ala-Azb and Rh-GABA-Azb, as shown for Rh- β -Ala-Azb in Fig. 1A, with $\lambda_{\text{max}} = 374$ nm and $\lambda_{\text{max}} = 371$ nm for Rh-GABA-Azb. Irradiation of either rhodium complex at a

wavelength of 375 nm converted *trans*-azobenzene to the *cis*-conformation, as evidenced by the shift of the $\pi \rightarrow \pi^*$ from 374 nm to 264 nm, consistent with the *cis*-conformation (Fig. 1A). The $n \rightarrow \pi^*$ ($\lambda_{\text{max}} \sim 500$ nm) also increased in intensity, consistent with the photolytic behavior of azobenzene.¹⁶ The dark *cis*-to-*trans* isomerization rate of Rh- β -Ala-Azb and Rh-GABA-Azb was significantly slower than for the uncomplexed 4,4'-diaminoazobenzene derivative, taking six to eight hours for complete relaxation to the *trans* conformation (Fig. 1B), compared to 15 minutes for the 4,4'-diaminoazobenzene starting compound. The longer relaxation time is expected based on the restricted flexibility of azobenzene when it is coupled on both ends in $[\text{Rh}(\text{PNR}^{\text{P}})_2]^+$. The complex with the two carbon chain, Rh- β -Ala-Azb relaxes slightly slower than Rh-GABA-Azb with a three carbon chain (Fig. 1B). This suggests more steric constraint in the two carbon chain Rh- β -Ala-Azb than in the three carbon chain Rh-GABA-Azb.

The structural isomerization of these complexes was also observed by ^1H NMR spectroscopy. Protons attached to the methylene carbons between the nitrogen and phosphorus (labeled 3 in Fig. 2) in Rh- β -Ala-Azb have inequivalent chemical shifts in the *cis*-conformation as opposed to the *trans*-conformation, where the same aliphatic protons are equivalent (Fig. 2). The rate of the *cis*-to-*trans* isomerization observed from ^1H NMR spectroscopy agrees with the rate obtained from UV/Vis absorption methods (Fig. S5 \dagger).

Computational structural characterization

To provide further insight into structural changes, computational studies of the complexes with azobenzene were evaluated and compared to $[\text{Rh}(\text{PN}^{\text{Gly-OH}})_2]^+$. The simulations show that in all cases the dihedral angle (the angle between the two planes defined by P-Rh-P and P'-Rh-P' (Fig. S8 \dagger)) at the metal center deviates from planarity, contrary to the crystal structure

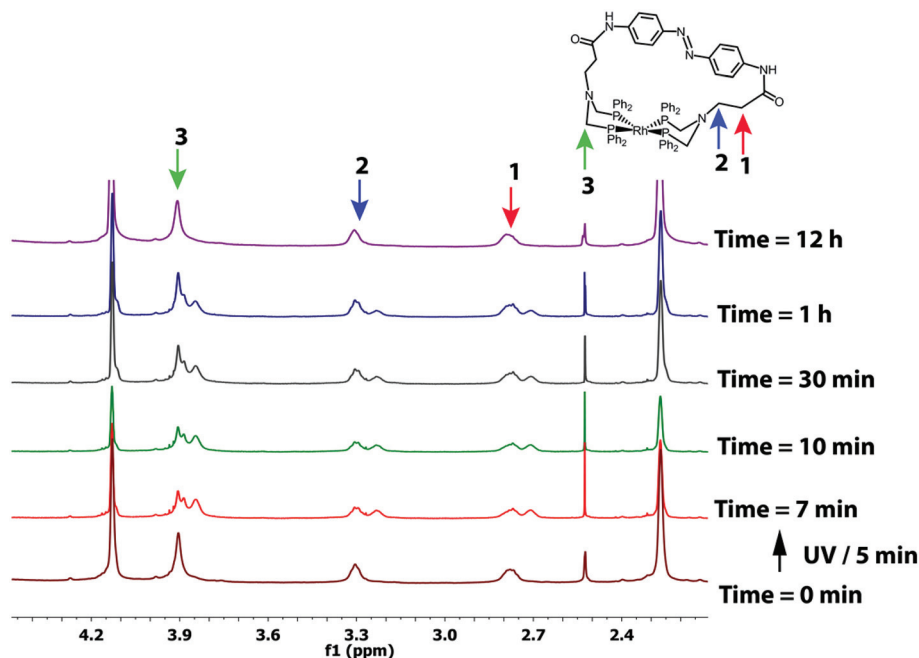


Fig. 2 ^1H NMR of Rh- β -Ala-Azb before (time = 0) and after (time = 7 minutes to 12 hours) 5 min of UV light irradiation. The three aliphatic proton resonances observed for the *trans*-isomer (time = 0) become inequivalent upon 5 min irradiation with UV light, resulting in three pairs of aliphatic proton resonances. This is indicative of a structural change and suggestive of an asymmetric structure due to the strain induced by the *cis* conformation of the azobenzene.

Table 1 Calculated structures for the azobenzene-containing rhodium complexes reported in this study. Additional parameters are reported in Table S1

Complex	\angle dihedral ^a ($^\circ$)	\angle P-Rh-P ($^\circ$)	\angle P'-Rh-P' ($^\circ$)	$r(\text{Rh-N})$ (\AA)
Rh- β -Ala-(<i>cis</i>)Azb	36.7 ± 8.4	89.2 ± 2.8	89.1 ± 3.0	9.2 ± 0.4
Rh- β -Ala-(<i>trans</i>)Azb	11.4 ± 5.2	90.0 ± 2.6	86.3 ± 2.5	6.8 ± 0.4
Rh-GABA-(<i>cis</i>)Azb	34.8 ± 9.0	90.1 ± 2.8	89.1 ± 2.8	9.6 ± 0.5
Rh-GABA-(<i>trans</i>)Azb	10.7 ± 5.2	90.0 ± 2.7	87.1 ± 2.6	6.7 ± 0.4
$[\text{Rh}(\text{PN}^{\text{Gly-OH}}\text{P})_2]^+$	9.8 ± 5.7	91.2 ± 2.6	89.7 ± 2.7	—

^aThe dihedral is the angle between the two planes P-Rh-P and P'-Rh-P'. $r(\text{Rh-N})$ is the distance between the Rh metal center and one of the N atoms in azo group in the Azb bridge (shown in Fig. 3).

isolated for $[\text{Rh}(\text{PN}^{\text{Gly-OH}}\text{P})_2]^+$,¹⁴ with an angle ~ 10 degrees in the $[\text{Rh}(\text{PN}^{\text{Gly-OH}}\text{P})_2]^+$ complex and in the *trans*-azobenzene isomers, and ~ 35 degrees for the *cis*-azobenzene-isomers (Table 1). The distances between the rhodium center and the nitrogen of the azo-bridge are also significantly different for the complexes in the *cis*- (dark) and *trans*- (light) conformations, with the azo-bridge in the *cis*-isomer giving a distance of ~ 9 \AA , and in the *trans*-isomer ~ 7 \AA (Table 1 and Fig. 3), in both cases too far from the rhodium to hinder activity *via* a direct interaction of the azo-group with rhodium. Changes in the bite angle (\angle P-Rh-P) were measured from the simulations, as it has been shown that small changes in this angle can significantly alter the electronics of the metal center.¹⁷ The pendant amines in the complexes were observed

to maintain the chair-chair conformation and the azo-bridge did not undergo *cis-trans* isomerization within a given simulation. Representative structures of the *cis* and *trans*-isomers are shown in Fig. 3.

Effect of the azobenzene photoswitch on the catalytic hydrogenation of CO_2

Each of the four metal complexes is active for CO_2 hydrogenation at 27 $^\circ\text{C}$. *N*-Methylpyrrolidinone (NMP) was used as the solvent to accommodate the limited solubility of the azobenzene-containing complexes. Catalytic reactions of CO_2 to formate were performed under 1 : 1 CO_2 : H_2 at 40 atm in a view cell composed of a stainless steel block reactor with a sapphire window in one side to allow photolysis of the sample. Catalytic activity of the azobenzene-containing complexes was evaluated both during constant irradiation with a 100 watt UV light ($\lambda_{\text{max}} = 365$ nm) and in the dark, where the dark experiments were performed irradiated, but with the window covered, to account for any thermal heating of the reactor. The catalytic production of formate was quantified by integrating the formate resonance in the ^1H NMR spectrum (8.7 ppm) with respect to the formamide resonance (8.0 ppm) of DMF added as an internal standard (see Table 2 and the Experimental section for details) The base 1,8-diazobicyclo[5.4.0]-undec-7-ene (DBU) was added to deprotonate the rhodium dihydride intermediate formed during the catalytic cycle, as well as to stabilize the formate from the reaction back to CO_2 and H_2 .

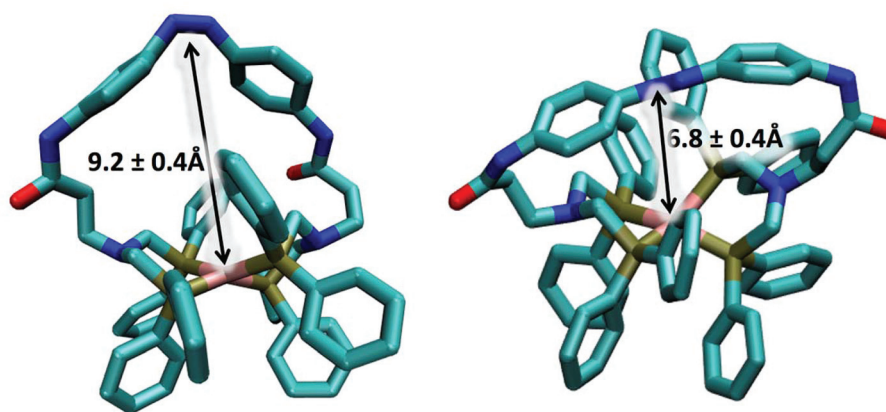


Fig. 3 Representative structures of the (left) *cis*- and (right) *trans*-azobenzene in Rh- β -Ala-Azb, showing the chair–chair conformation maintained by the pendant amine in both complexes, as well as the average distance of the azo-group from the rhodium.

Table 2 Rates of CO₂ hydrogenation for [Rh(PN^RP)₂]⁺ and Rh-R-Azb complexes. Rates for the azobenzene containing complexes were determined in the *cis*-azobenzene (light) and *trans*-azobenzene (dark) conformations

Catalyst	[M ⁺] (mM)	[DBU] (mM)	Azobenzene conformation	TOF (h ⁻¹)	TON ^a (TON ^b)
[Rh(PN ^{β} -Ala-OH-P) ₂] ⁺	1.5	700	—	33 ± 3	790 (890)
[Rh(PN ^{GABA} -OH-P) ₂] ⁺	1.5	800	—	32 ± 2	770 (910)
Rh-β-Ala-Azb	1.2	420	<i>cis</i>	16 ± 2	380 (600)
			<i>trans</i>	11 ± 2	280 (630)
Rh-GABA-Azb	1.1	420	<i>cis</i>	17 ± 0.2	410 (710)
			<i>trans</i>	18 ± 0.2	430 (720)

All the reactions were carried out in *N*-methyl-pyrrolidinone, catalyst concentration 1.1–1.5 mM, 27 °C, either light or dark, for 24 hours. All data are an average of three runs, except [Rh(PN ^{β} -Ala-OH-P)₂]⁺ which is an average of two runs. ^aThe TON was calculated experimentally. ^bThe theoretical TON is based on added DBU and the formate:DBU (1.7) due to homoassociation (see Experimental section and Fig. S6 for details).

Thermodynamic studies

To evaluate mechanistic steps in the catalytic cycle, stoichiometric studies of H₂ addition and subsequent deprotonation of all four complexes were carried out under similar solvent conditions to those used for catalysis. The dihydrides resulting from H₂ addition (1 atm), [H₂Rh(PN^RP)₂]⁺ and H₂Rh-R-Azb were identified by two doublets of triplets in the ¹H NMR with the typical AA'XX'M splitting pattern observed for these complexes.¹⁴ Representative ¹H and ³¹P{¹H} NMR spectra for Rh- β -Ala-Azb are shown in Fig. 4.¹⁸ As captured in the *K*_{eq} values, the Rh- β -Ala-Azb formed significantly more dihydride than the non-azobenzene counterpart ([Rh(PN ^{β} -Ala-OH-P)₂]⁺), while the opposite trend was observed for the GABA containing complexes (Table 3). In all cases, addition of ~50 eq. DBU to the above dihydride complexes quantitatively converted to a monohydride, [HRh(PN^RP)₂]⁺, containing a single broad (too broad to observe Rh–H coupling) resonance in the ¹H NMR spectra and a doublet due to rhodium coupling in the ³¹P{¹H}

Table 3 Thermodynamic parameters for the reaction of [Rh(PN^RP)₂]⁺ or Rh-R-(*trans*)-Azb (dark) with H₂ to produce the dihydride complexes, [H₂Rh(PN^RP)₂]⁺ or H₂-Rh-R-(*trans*)-Azb

Complex	<i>K</i> _{eq} (atm ⁻¹)	ΔG_{H_2} (kcal mol ⁻¹)
[H ₂ Rh(dppp) ₂]	6.70 ^a	-1.10 ^a
[H ₂ Rh(PN ^{Gly} -OH-P) ₂]	0.30 ^a	+0.77 ^a
[H ₂ Rh(PN ^{β} -Ala-OH-P) ₂]	0.53	+0.37
[H ₂ Rh(PN ^{GABA} -OH-P) ₂]	1.71	-0.32
H₂Rh-β-Ala-Azb	1.48	-0.23
H₂Rh-GABA-Azb	0.97	+0.02

^a Reported in ref. 14. All H₂ additions were carried out in a J. Young NMR tube at 1 atm H₂. The units for *K*_{eq} result from the concentration of H₂ gas which is not 1 M (*i.e.* non-standard state).

NMR spectra, consistent with a square pyramidal structure containing four equivalent phosphorous atoms. Repeating these experiments under light conditions (*cis*-azobenzene configuration) produced the same distribution of intermediates.

Discussion

Enzymes have long been known to control catalysis by altering their dynamic structure.^{1a} Mimicking this feature in molecular catalysts has the potential to provide similar regulation in molecular complexes, and could include additional advantages such as protecting the catalyst from poisons or modulating catalytic activity between different substrates. In this work, we exploit the structural interconversion of azobenzene by binding azobenzene across a rhodium center to produce a photo-responsive tetradentate ligand, to investigate the impact on catalytic activity.

To investigate the role of structural switching on catalytic activity, we prepared rhodium complexes with an azobenzene-derived (bis)diphosphine photo-responsive tetradentate ligand, Rh-R-Azb. This ligand motif is similar to those observed in *trans*-spanning ligands. The first *trans*-spanning

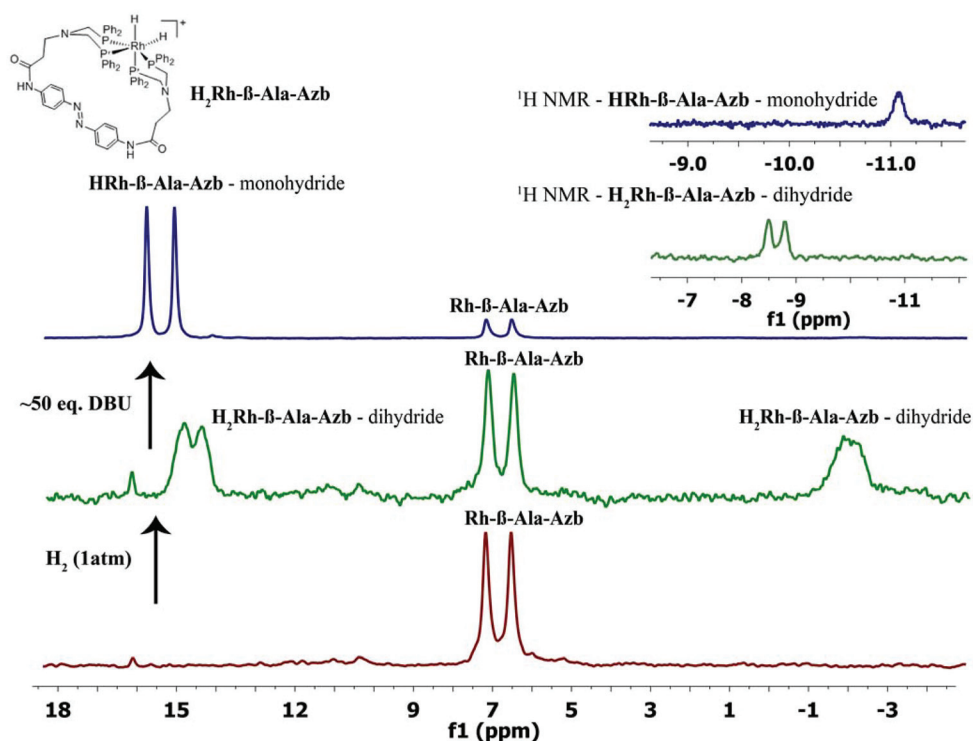


Fig. 4 The $^{31}\text{P}\{^1\text{H}\}$ NMR spectra of $\text{Rh-}\beta\text{-Ala-Azb}$ (bottom), $\text{H}_2\text{Rh-}\beta\text{-Ala-Azb}$ (middle) and $\text{HRh-}\beta\text{-Ala-Azb}$ (top). One atm H_2 was added using a J. Young NMR tube with 10 mM complex in NMP. Upper right shows the ^1H NMR of the hydride resonance for the monohydride and dihydride of $\text{Rh-}\beta\text{-Ala-Azb}$.

ligand reported by Issleib and Hohlfield in 1961 was based on an alkyl chain bridged diphosphine ligand $(\text{C}_6\text{H}_{11})_2\text{P}(\text{CH}_2)_n\text{-P}(\text{C}_6\text{H}_{11})_2$ which yielded distorted square planer geometries when bound to nickel with $n < 4$.¹⁹ Development of *trans*-spanning ligands is based on understanding and modulating the steric and electronic effects of the specific ligands.^{15,20} The incorporation of azobenzene into the $[\text{Rh}(\text{PN}^{\text{R}}\text{P})_2]^+$ complexes discussed here imposes a similar structural strain on the macrocycle formed, and additionally provides the opportunity to toggle between two differently strained structures.

The $\text{Rh-}\beta\text{-Ala-Azb}$ complex showed a difference in CO_2 hydrogenation activity under *cis*- and *trans*-conformational forms. The complex with the azobenzene in the *cis*-conformation showed a 40% rate enhancement compared to the complex with the azobenzene in the *trans*-conformation, indicating that the photoinitiated structure is altering the active site in some way to influence reactivity. Dependence upon chain length is demonstrated in that the Rh-GABA-Azb complex with an additional carbon does not exhibit a difference in rate between the *cis*- and *trans*-conformations. Attempts to look at an even shorter carbon chain, *i.e.* glycine, did not result in the tetradentate ligand with the azobenzene bridge, but instead resulted in a complex with an azobenzene attached to each glycine, preventing further evaluation of the chain length (See ESI† for details).

The parent rhodium complexes, $[\text{Rh}(\text{PN}^{\beta\text{-Ala-OH}}\text{P})_2]^+$ and $[\text{Rh}(\text{PN}^{\text{GABA-OH}}\text{P})_2]^+$, were also investigated for comparison and

showed rates two-times higher compared to the azobenzene cross-linked derivatives (Table 2), attributed to the free acidic functionality as previously reported.¹⁴ This suggests several factors which may be contributing to reactivity: (1) the azobenzene could change the geometry of the active site for $\text{Rh-}\beta\text{-Ala-Azb}$ altering the electronics and/or thermodynamics; (2) the nitrogen groups of the azo functional group could bind to the metal in the *trans*-configuration, hindering reactivity.

Crystal structures have the potential to reveal structural contributions of the azobenzene ligands to the reactivity, but unfortunately we were unable to obtain crystals of these complexes. To provide insight into which of these possibilities might be dominating the reactivity of these complexes, we performed semi-empirical calculations on the azobenzene-containing complexes and $[\text{Rh}(\text{PN}^{\text{Gly-OH}}\text{P})_2]^+$. These calculations demonstrate that azobenzene is too far from the metal to bind in either the *cis*- or *trans*-conformations, removing azobenzene metal binding as a possible explanation of the differences in observed rates. Significant differences in structure are observed between *cis*- and *trans*-conformations, particularly in the dihedral angle and the Rh-N distances, but not between the complexes with different carbon length linkers, suggesting that *significant* structural changes are not contributing to the observed catalytic behavior. Further, because large changes are observed in the dihedral angle between *cis* and *trans* for both complexes, this suggests that reactivity for CO_2 is not sensitive to these angular and spatial parameters.

It is also possible that the azobenzene is contributing directly to steps in the catalytic cycle, such as H₂ addition or deprotonation. To understand potential changes in thermodynamics, intermediates in two of the three steps in the proposed catalytic cycle (Fig. S1†) were prepared. The dihydride was formed by exposure to H₂, and deprotonation to form the monohydride was achieved by the addition of DBU. **Rh-β-Ala-Azb** and **Rh-GABA-Azb** have negative or zero values for ΔG_{H₂}, resulting in favorable H₂ addition, similar to other [Rh(PN^RP)₂]⁺ complexes in this work and many that are reported earlier.¹⁴ Complete conversion to the hydride upon addition of base for all complexes, as well as a lack of correlation between the rate of H₂ addition and CO₂ hydrogenation, suggest that H₂ addition is not the rate limiting step in the mechanism, in agreement with the previously reported behavior.¹⁴ Importantly, the variability between the ΔG_{H₂} of these and previous complexes, with no correlation to activity, suggests that H₂ addition and subsequent deprotonation are not contributing to the differences observed in rates for the complexes in this study.

Collectively, the computational and thermodynamics results suggest that the azobenzene groups are not providing a significant structural change, or in the energetics of the intermediates in the catalytic cycle. Complexes similar to these have been shown to be extremely sensitive to small changes in hydricity, which can arise from subtle changes in the P–Rh–P bite angle. For example, ~10 degree changes in the bite angle for Co, Rh, Ir, Ni, Pt or Pd complexes results in ~20 kcal mol⁻¹ change in the hydricity, or ~2 kcal per mol per degree.^{17a} The modest changes in rate observed here are consistent with a ΔΔG of 0.25 kcal mol⁻¹ or a change in bite angle of only 0.5 degrees, a change that is within the error of our calculations.

In summary, the introduction of an azobenzene across Rh(bis)diphosphine complexes allowed us to photolytically control the rate of CO₂ hydrogenation. This was only true in the complex with the shorter chain length (**Rh-β-Ala-Azb**), suggesting a steric component to the catalytic control. Computational data suggest that the large changes in structure due to *cis*–*trans* isomerization (*i.e.* dihedral and *r*(Rh–N)) are not responsible for the differences in rate. Consistent with both the experimental and computational data is that the steric rigidity is introducing subtle changes in the P–Rh–P bite angle for **Rh-β-Ala-Azb**, resulting in a change in hydricity, controlling catalysis. This behavior is inspired by enzymatic regulation of catalytic processes, and demonstrates that similar control is possible for molecular complexes.

Experimental

General methods

All chemical reactions were performed under inert atmosphere on a Schlenk line or in a glove box unless otherwise noted. All the reagents were purchased from Sigma Aldrich and used without further purification. DBU (1,8-diazabicyclo[5.4.0]-undec-7-ene) was degassed by repeated freeze–pump–thaw

cycles before use. Tetrahydrofuran (*d*₈-THF) from Cambridge isotope was dried over NaK and vacuum transferred. Other organic solvents were dried and degassed using an Innovative Technology, Inc., PureSolv Solvent purification systems. UHP (ultra-high purity) CO₂ and H₂ were purchased from Oxarc. ¹H and ¹³C{¹H} NMR spectra were recorded on Varian Inova 500 MHz or VNMRs 300 MHz NMR spectrometers. All ¹H chemical shifts are internally calibrated using the monoprotic impurity of the deuterated solvent; ¹³C NMR chemical shifts are referenced to CD₃CN or *d*₈-THF. ³¹P{¹H} NMR spectra were obtained on a Varian Inova 500 spectrometer and are referenced externally to 85% H₃PO₄ (0 ppm). Mass analysis was performed using a 15T Fourier transform ion cyclotron resonance mass spectrometer (FTICR-MS) (Bruker Solarix, Billerica, MA) outfitted with a standard electrospray ionization (ESI) interface. UV-Vis spectra of azobenzene derivatives were measured on Shimadzu UV-2401PC UV-Vis spectrometer. Isomerization of these samples from *trans* to *cis* was achieved with a 1000 watt xenon–mercury arc lamp, directed through a monochromator to generate light at λ = 375 nm. Catalytic studies of the azobenzene bound complexes were performed using the 100 watt UV lamp, UVP-B100 series with a peak intensity (21 700 μW cm⁻² at 2" distance) at 365 nm and a distribution of ±40 nm. (The 100 watt UV lamp was used for catalysis after determining the rates (~5 minutes) of *trans*–to–*cis* conversion of the complexes by both lamps were similar.)

The rates of the *cis*–to–*trans* isomerization of **Rh-β-Ala-Azb** and **Rh-GABA-Azb** were determined by monitoring the increase in the π to π* absorption band at 365 nm after irradiation. Rate constants for isomerization were determined by fitting the data to a first order rate equation.

Preparation of PN^{β-Ala-OH}P

A 250 mL Schlenk flask was loaded with 0.081 g (2.69 mmol) paraformaldehyde, 0.5 g (2.69 mmol) diphenylphosphine, and β-alanine (0.119 g, 1.34 mmol) in 150 mL ethanol. The reaction flask was heated to 70 °C and stirred for 12 hours. After 12 hours the solvent was removed under reduced pressure to obtain a viscous oil. The oil was dissolved in 2–3 mL of THF and the white product was precipitated using diethyl ether. The solid was filtered through a medium frit and thoroughly washed with diethyl ether to obtain a white solid in 85% yield. ¹H NMR (500 MHz, CD₃CN): δ 2.37 (br, 2H, NCH₂CH₂COOH), 3.14 (br, 2H, NCH₂CH₂COOH), 3.65 (s, 4H, PCH₂N), 6.96–8.06 (m, 20H, P-PhH), 10.82 (br, 1H, N–CH₂CH₂COOH). ¹³C{¹H} NMR (125 MHz, CDCl₃): δ 30.3 (–CH₂–COOH), 51.9 (N–CH₂–CH₂), 57.7, 128.9 (s, C-Ph), 129.3 (s, C-Ph), 133.2 (d, ²J_{PC} = 19 Hz, C-Ph), 136.8 (d, ¹J_{PC} = 10.7 Hz, C-Ph), 173.9 (–CH₂–COOH). ³¹P{¹H} NMR (202 MHz, *d*₈-THF): δ –29.15. ESI MS: observed (MH⁺) *m/z* = 486.17; calculated (MH⁺) *m/z* = 486.17. Elem. anal. Calcd for C₂₉H₂₉NO₂P₂ + 0.5diethyl ether: C, 71.25; H, 6.56; N, 2.68; Found C, 71.10; H, 6.35; N, 2.73.

Preparation of PN^{GABA-OH}P

This ligand was prepared in a similar manner to PN^{β-Ala-OH}P with 0.74 g (7.14 mmol) γ-aminobutyric acid (GABA), 2.67 g

(14.3 mmol) diphenylphosphine and 0.50 g paraformaldehyde in 150 mL ethanol and stirred for 16 h at 71 °C. Removal of solvent produced an oily material. This was then dissolved in minimal THF (~1–2 ml) and added dropwise to 10 ml of diethyl ether to produce a white precipitate. The white solid was isolated upon filtration and washed with excess diethyl ether and dried under vacuum to obtain a white solid in good yield, ~82%. ¹H NMR (500 MHz, *d*₈-THF): δ 1.33 (br, 2H, NCH₂CH₂CH₂COOH), 1.69 (br, 2H, NCH₂CH₂CH₂COOH), 2.33 (br, 2H, NCH₂CH₂CH₂COOH), 3.29 (s, 4H, PCH₂N), 7.10–7.33 (m, 20H, PPhH), 8.82 (br, 1H, NCH₂CH₂COOH). ¹³C{¹H} NMR (125 MHz, CDCl₃): δ 21.9 (CH₂–CH₂–CH₂), 30.7 (CH₂–CH₂–CH₂), 32.0 (CH₂–CH₂–CH₂), 58.7 (P–CH₂–N), 128.5 (C-Ph), 129.2 (C-Ph), 133.1 (*d*, ²J_{PC} = 17.5, C-Ph), 137.9 (*d*, ¹J_{PC} = 12.5, C-Ph). ³¹P{¹H} NMR (202 MHz, CD₃CN): δ –26.7. ESI MS: observed (MH⁺) *m/z* = 500.19; calculated (MH⁺) *m/z* = 500.18. Elem anal. Calcd for C₃₀H₃₁NO₂P₂ + 0.5diethyl ether: C, 71.63; H, 6.76; N, 2.61; Found C, 71.66; H, 6.44; N, 2.81.

General procedure for the synthesis of [Rh(PN^RP)₂]⁺

To a solution of the PN^RP ligand (1 mmol) in THF, 0.5 mmol of Rh(COD)₂OTf was added drop wise to a 20 mL glass vial equipped with a stir bar. This solution was stirred for 12 h to obtain a clear yellow solution. The THF solution was concentrated to 1 mL under reduced pressure and was added drop wise to a flask containing 10 mL diethyl ether to precipitate the product as a yellow suspension. The product was filtered through a medium frit, the solid was thoroughly washed with diethyl ether and dried to afford the Rh complex in good yield (70–85%).

[Rh(PN^{β-Ala-OH}P)₂](OTf)

The compound was prepared following the above procedure at a 1 mmol ligand scale to obtain a yellow solid in 70% yield. ¹H NMR (500 MHz, CD₃CN): δ 2.11 (t, 4H, J_{HH} = 8 Hz, CH₂CH₂COOH), 2.66 (t, 4H, J_{HH} = 8 Hz, NCH₂CH₂COOH), 3.36 (s, 8H, PCH₂N), 7.10–7.55 (m, 40H, PPhH), 9.16 (br, 2H, NCH₂CH₂COOH); ¹³C{¹H} NMR (125 MHz, *d*₆-DMSO): δ 33.9, 35.2 (–CH₂CH₂C(O)), 60.7 (P–CH₂–N) 119.9, 123.9, 142.0, 148.15 (aromatics) 169.3, (COOH); ³¹P{¹H} NMR (202 MHz, *d*₈-THF): δ 8.38, J_{RhP} = 130.1 Hz. ESI MS: observed (M⁺ – OTf) *m/z* = 1073.24; calculated (M⁺ – OTf) *m/z* = 1072.31. Elem anal. Calcd for C₅₉H₅₈N₂O₇F₃P₄RhS: C, 57.94; H, 4.78; N, 2.29; Found C, 57.70; H, 4.90; N, 2.30.

[Rh(PN^{GABA-OH}P)₂](OTf)

Following the general procedure above, [Rh(PN^{GABA-OH}P)₂]⁺ compound was prepared as a yellow solid in 85% yield. ¹H NMR (500 MHz, *d*₈-THF): δ 1.28 (br, 4H, NCH₂CH₂CH₂COOH), 1.64 (br, 4H, NCH₂CH₂CH₂COOH), 2.28 (br, 4H, NCH₂CH₂CH₂COOH), 3.24 (s, 8H, PCH₂N), 6.92–7.49 (m, 40H, PPhH); ³¹P{¹H} NMR (202 MHz, CD₃CN): δ 8.43 (*d*, J_{RhP} = 131.3 Hz). ¹³C{¹H} NMR (125 MHz, 10% D₂O and *d*₈-THF): δ 21.2, (NCH₂CH₂CH₂–), 29.5, (NCH₂CH₂–CH₂–), 33.4, (NCH₂CH₂–CH₂–), 55.0 (br, PCH₂N), 126.1, 126.3, 131.9, 142.1 (aromatics) 175.1 (–CONH) ESI MS: observed (M⁺ – OTf) *m/z* = 1101.27;

calculated (M⁺ – OTf) *m/z* = 1101.25. Elem anal. Calcd for C₆₁H₆₂N₂O₇F₃P₄RhS + 1H₂O: C, 57.69; H, 5.16; N, 2.21; Found C, 57.43; H, 5.17; N, 2.22.

Rh-β-Ala-Azb

A 250 mL schlenk flask containing 0.2 g (0.16 mmol) [Rh(PN^{β-Ala-OH}P)₂](OTf) and 2.2 equivalent HATU (0.124 g, 0.33 mmol) in 100 mL THF was stirred and diisopropylethyl amine (DIPEA) (0.046 g, 0.36 mmol) was added to the flask. This solution was stirred for 15 minutes and diaminoazobenzene (0.035 g, 0.16 mmol) dissolved in 5 mL of THF was added drop wise in the dark to the above reaction solution and stirred for 24 hours under ambient light. Removal of solvent resulted in a yellow powder which was redissolved in 2–3 mL of 5–10% aqueous THF and precipitated into 15 mL of diethyl ether. This precipitate was filtered through a medium frit, the yellow solid was washed thoroughly with diethyl ether followed by washing with acetonitrile to obtain a bright yellow solid in 42% yield, which has a ~50:50 mixture of triflate and hexafluorophosphate counterions (if excess HATU was used for the synthesis of the above complex, total exchange of the OTf to PF₆ was observed. The rates for CO₂ hydrogenation with a single counter anion or mixed counter anions did not show a significant difference (Table S3[†]). ¹H NMR (500 MHz, 10% D₂O and *d*₈-THF): δ 2.30 (br, 4H, NCH₂CH₂CONH), 2.83 (br 4H, NCH₂CH₂CONH), 3.43 (s, 8H, PCH₂N), 6.74–7.91 (m, 48H, PPhH & Azb-PhH); ¹³C{¹H} NMR (125 MHz, 10% D₂O and *d*₈-THF): δ 31.22, (NCH₂CH₂–), 33.37, (NCH₂CH₂–), 57.18 (br, PCH₂N), 119.3, 123.3, 128.2, 130.1, 131.0, 132.2, 132.8, 133.3, (aromatics) 169.9 (–CONH); ³¹P{¹H} NMR (202 MHz, 10% D₂O and *d*₈-THF): δ 7.93 (*d*, J_{RhP} = 130.3 Hz). ESI MS: observed (MH⁺ – OTf) *m/z* = 1251.325; calculated (MH⁺ – OTf) *m/z* = 1250.32. Elem anal. Calcd for C₇₀H₆₆F₆N₆O₂P₅Rh: C, 60.27; H, 4.77; N, 6.02; Found C, 60.05; H, 4.90; N, 6.33.

Rh-GABA-Azb was prepared following a similar procedure as described above with 0.25 g of [Rh(PN^{GABA-OH}P)₂]⁺ to obtain a bright yellow solid in 40% yield, with a ~50:50 mixture of triflate and hexafluorophosphate counterions. ¹H NMR (500 MHz, 10% D₂O and *d*₈-THF): δ 1.52 (br 4H, NCH₂CH₂CH₂CONH), 2.06 (br 4H, NCH₂CH₂CH₂CONH), 2.47 (br 4H, NCH₂CH₂CH₂CONH), 3.38 (s, 8H, PCH₂N), 6.72–7.79 (m, 48 H, PPhH & AzbPhH); ¹³C{¹H} NMR (125 MHz, CD₃CN): δ 25.7, 27.3, 33.9, (–CH₂CH₂CH₂–), 60.9, (PCH₂N–), 119.0, 119.3, 123.2, 123.4, 141.9, 147.4, 157.4, (aromatics) 171.5 (CONH); ³¹P{¹H} NMR (202 MHz, CD₃CN): δ 7.07 (*d*, J_{RhP} = 131 Hz). ESI MS: observed (MH⁺ – OTf) *m/z* = 1278.34; calculated (MH⁺ – OTf) *m/z* = 1278.36. Elem anal. Calcd for C₇₂H₇₀F₆N₆O₂P₅Rh + 4THF + 3H₂O: C, 60.92; H, 5.34; N, 4.79; Found C, 60.75; H, 5.07; N, 4.63.

General procedure for catalysis

The high-pressure view cell, previously reported,²¹ having a sapphire optical window with a teflon o-ring seal and one gas port, was used for all batch CO₂-hydrogenation reactions. The cell was sufficient to contain the 40 atm of CO₂/H₂ used for catalysis at room temperature. This window was used to

irradiate the sample with UV light to control the conformation of the azobenzene in the complex and to provide a means of viewing the reaction solution during catalysis.

The reaction solution was prepared in a glove box under N₂ atmosphere and the catalyst and DBU base were dissolved in 1.0 mL of *N*-methylpyrrolidinone (NMP) which was then added to the high-pressure view cell. The volume was then adjusted to a total volume between 3.0 mL to 3.5 mL with NMP to result in final catalyst concentrations of 1.1 mM–1.5 mM and final DBU concentrations of 410–650 mM. No difference in rate was observed for a given catalyst under similar conditions within this concentration range. The reaction cell was connected to a model 500D ISCO syringe pump apparatus *via* PEEK tubing, and an N₂ environment in the tubing were eliminated by applying a pseudo vacuum (connected to the vacuum when active vacuum valve is closed).¹⁴ Then the 1:1 CO₂/H₂ gas mixture was delivered at a constant pressure of 40 atm using an ISCO syringe pump. Following this addition, the reaction proceeded for 24 hours with stirring to allow for gas mixing with the liquid phase during catalysis. UV light was kept turned “ON” even for dark reaction conditions where the viewport was closed with a black aluminum foil to account for any thermal fluctuations in the “dark” and “light” states. The temperature of the pressure vessel was monitored using an external thermocouple, and recorded to be 27 ± 1 °C in all catalytic reactions, both light and dark. A 10–20% loss of the complex in the *trans*-conformation was observed after 24 hours under catalytic conditions, performed under either light or dark conditions.

Determination of TONs

After 24 hours, the view cell and PEEK tubing were disconnected from the CO₂:H₂ gas inlet and the pressure was released in the glove box. 300 μL aliquots of the reaction solution were placed in an NMR tube to which 50 μL aqueous 10% *N,N*-dimethylformamide (DMF) was added. The determination of TONs for the catalytic runs were carried out by integrating the formate resonance with respect to the formamide proton of DMF in the ¹H NMR spectrum which was run with an acquisition time of 2 s, a 1 s relaxation delay, and 100 scans. The TOF's reported in Table 2 were calculated for reactions after 24 h using the following equation:

$$\text{TOF} = \frac{[\text{formate}]}{[\text{catalyst}] \times 24(\text{h})}$$

and the value reported is an average of three experiments run under identical conditions, with the exception of [Rh(PN^{β-Ala-OH}P)₂]⁺ which is an average of only two experiments. The theoretical TON was calculated using the following equation:

$$\text{TON} = \frac{[\text{DBU}] \times 1.7}{[\text{catalyst}]}$$

where the formate:DBU homoassociation was found to be ~1.7, which was determined by adding formic acid to a known

concentration of DBU in NMP and monitoring the required amount of formic acid to consume the DBU (Fig. S6†).

Thermodynamic studies

Addition of H₂ to the [Rh(PN^RP)₂]⁺ complexes was carried out in J. Young NMR tubes. The metal complex was dissolved in 400 μL of NMP and added to the NMR tube in a N₂ atmosphere. On a gas manifold, the N₂ atmosphere in the NMR tube was removed by exposing it to the static vacuum in the manifold three times. This involved pulling the vacuum on the gas manifold with the J. Young tube closed, isolating the manifold from the vacuum pump, and then opening the J. Young tube to the static vacuum in the manifold. Hydrogen was added similarly by exposing the solution in the J. Young tube to 1 atm hydrogen three times, with one minute of vortex mixing between each addition.

Computational studies

Stable structures were optimized starting from the crystal structures of [Rh(PN^{Gly-OH}P)₂]⁺ using a semi-empirical level of theory (PM6).²² The lowest energy structure was selected (see ESI of ref. 14) and molecular dynamics studies were carried out in the gas phase to explore the structural parameters of the *cis*-azobenzene and *trans*-azobenzene within the complexes, for both the **Rh-β-Ala-Azb** and **Rh-GABA-Azb**. All simulations were performed using the CP2K program²³ and trajectories were generated using the NVT ensemble at 300 K. Data were collected for 75 ps of simulation time. The initial structures in the simulations were in the chair–chair configuration, as that configuration was found to be most stable.

Acknowledgements

This work was supported by the US Department of Energy, Office of Science, Office of Basic Energy Sciences, Division of Chemical Sciences, Geosciences & Biosciences. Pacific Northwest National Laboratory (PNNL) is a multiprogram national laboratory operated for the DOE by Battelle. A portion of this research was performed using EMSL, a national scientific user facility sponsored by the Department of Energy's Office of Biological and Environmental Research and located at Pacific Northwest National Laboratory.

References

- (a) A. Gora, J. Brezovsky and J. Damborsky, Gates of enzymes, *Chem. Rev.*, 2013, **113**(8), 5871–5923; (b) J. Lee and N. M. Goodey, Catalytic contributions from remote regions of enzyme structure, *Chem. Rev.*, 2011, **111**(12), 7595–7624.
- (a) J. C. Boyington, V. N. Gladyshev, S. V. Khangulov, T. C. Stadtman and P. D. Sun, Crystal structure of formate dehydrogenase H: catalysis involving Mo, molybdopterin, selenocysteine, and an Fe₄S₄ cluster, *Science*, 1997, **275**(5304),

- 1305–1308; (b) H. C. Raaijmakers and M. J. Romao, Formate-reduced *E. coli* formate dehydrogenase H: The reinterpretation of the crystal structure suggests a new reaction mechanism, *J. Biol. Inorg. Chem.*, 2006, **11**(7), 849–854.
- 3 (a) K. A. Henzler-Wildman, V. Thai, M. Lei, M. Ott, M. Wolf-Watz, T. Fenn, E. Pozharski, M. A. Wilson, G. A. Petsko, M. Karplus, C. G. Hubner and D. Kern, Intrinsic motions along an enzymatic reaction trajectory, *Nature*, 2007, **450**(7171), 838–844; (b) E. Z. Eisenmesser, O. Millet, W. Labeikovsky, D. M. Korzhnev, M. Wolf-Watz, D. A. Bosco, J. J. Skalicky, L. E. Kay and D. Kern, Intrinsic dynamics of an enzyme underlies catalysis, *Nature*, 2005, **438**(7064), 117–121.
- 4 K. A. Henzler-Wildman, M. Lei, V. Thai, S. J. Kerns, M. Karplus and D. Kern, A hierarchy of timescales in protein dynamics is linked to enzyme catalysis, *Nature*, 2007, **450**(7171), 913–916.
- 5 D. E. Bergbreiter, Using Soluble Polymers To Recover Catalysts and Ligands, *Chem. Rev.*, 2002, **102**(10), 3345–3384.
- 6 (a) C. Baleizao and H. Garcia, Chiral salen complexes: an overview to recoverable and reusable homogeneous and heterogeneous catalysts, *Chem. Rev.*, 2006, **106**, 3987–4043; (b) T. J. Dickerson, N. N. Reed and K. D. Janda, Soluble polymers as scaffolds for recoverable catalysts and reagents, *Chem. Rev.*, 2002, **102**, 3325–3344; (c) N. Madhavan, C. W. Jones and M. Weck, Rational approach to polymer-supported catalysts: synergy between catalytic reaction mechanism and polymer design, *Acc. Chem. Res.*, 2008, **41**, 1153–1165.
- 7 (a) W. J. Shaw, Y. Chen, J. Fulton, J. Linehan, A. Gutowska and T. Bitterwolf, Structural evolution of a recoverable rhodium hydrogenation catalyst, *J. Organomet. Chem.*, 2008, **693**(12), 2111–2118; (b) W. J. Shaw, J. C. Linehan, A. Gutowska, D. Newell, T. Bitterwolf, J. L. Fulton, Y. Chen and C. F. Windisch, Synthesis and characterization of a recoverable rhodium catalyst with a stimulus sensitive polymer ligand, *Inorg. Chem. Commun.*, 2005, **8**(10), 894–896.
- 8 N. C. Gianneschi, P. A. Bertin, S. T. Nguyen, C. A. Mirkin, L. N. Zakharov and A. L. Rheingold, A Supramolecular Approach to an Allosteric Catalyst, *J. Am. Chem. Soc.*, 2003, **125**(35), 10508–10509.
- 9 L. Fabbrizzi, M. Licchelli and P. Pallavicini, Transition metals as switches, *Acc. Chem. Res.*, 1999, **32**, 846–853.
- 10 M.-a. Haga, T. Takasugi, A. Tomie, m. Ishizuya, T. Yamada, M. D. Hossain and M. Inoue, Molecular design of a proton-induced molecular switch based on rod-shaped Ru dinuclear complexes with bis-tridentate 2,6-bis(benzimidazol-2-yl)pyridine derivatives, *Dalton Trans.*, 2003, 2069–2079.
- 11 (a) G. Knor, Bionic catalyst design: a photochemical approach to artificial enzyme function, *ChemBioChem*, 2001, **7**(8), 593–596; (b) K. Okamoto, T. Yamamoto, M. Akita, A. Wada and T. Kanbara, Chemical stimuli induced phosphorescence modulation of secondary thioamide-based pincer platinum complexes, *Organometallics*, 2009, **28**, 3307–3310.
- 12 (a) B. M. Neilson and C. W. Bielawski, Illuminating Photo-switchable Catalysis, *ACS Catal.*, 2013, **3**(8), 1874–1885; (b) S. Umeki, S. Kume and H. Nishihara, Switching of molecular insertion in a cyclic molecule via photo- and thermal isomerization, *Inorg. Chem.*, 2011, **50**, 4925–4933; (c) A. Panja, t. Matsuo, S. Magao and S. Hirota, DNA cleavage by the photocontrolled cooperation of ZnII centers in an azobenzene-linked dizinc complex, *Inorg. Chem.*, 2011, **50**, 11437–11445; (d) J. Yin, G.-A. Yu, J. Guan, F. Mei and S. H. Liu, Synthesis and properties of conjugated bimetallic ruthenium complexes with s,s-bridging azobenzene chains, *J. Organomet. Chem.*, 2005, **690**, 4265–4271; (e) Y.-X. Yuan, Y. Chen, Y.-C. Wang, C.-Y. Su, S.-M. Liang, H. Chao and L.-N. Ji, Redox responsive luminescent switch based on a ruthenium(II) complex [Ru(bpy)2(PAIDH)]²⁺, *Inorg. Chem. Commun.*, 2008, **11**, 1048–1050; (f) Y. Yamamoto, H. Nakamura and J.-F. Ma, Preparation and characterization of ruthenium(II), rhodium(III) and iridium(III) complexes of isocyanide bearing the azo group, *J. Organomet. Chem.*, 2001, **640**, 10–20.
- 13 A. Ueno, K. Takahashi and T. Osa, Photocontrol of catalytic activity of capped cyclodextrin, *J. Chem. Soc., Chem. Commun.*, 1981, (3), 94–96.
- 14 J. T. Bays, N. Priyadarshani, M. S. Jeletic, E. B. Hulley, D. L. Miller, J. C. Linehan and W. J. Shaw, The influence of the second and outer coordination spheres on Rh(diphosphine)₂ CO₂ hydrogenation catalysts, *ACS Catal.*, 2014, **4**(10), 3663–3670.
- 15 C. A. Bessel, P. Aggarwal, A. C. Marschilok and K. J. Takeuchi, Transition-Metal Complexes Containing trans-Spanning Diphosphine Ligands, *Chem. Rev.*, 2001, **101**(4), 1031–1066.
- 16 H. M. D. Bandara and S. C. Burdette, Photoisomerization in different classes of azobenzene, *Chem. Soc. Rev.*, 2012, **41**(5), 1809–1825.
- 17 (a) X.-J. Qi, Y. Fu, L. Liu and Q.-X. Guo, Ab initio calculations fo thermodynamic hydricities of transition-metal hydrides in acetonitrile, *Organometallics*, 2007, **26**, 4197–4203; (b) X.-J. Qi, L. Liu, Y. Fu and Q.-X. Guo, Ab Initio Calculations of pKa Values of Transition-Metal Hydrides in Acetonitrile, *Organometallics*, 2006, **25**(25), 5879–5886; (c) M. R. Nimlos, C. H. Chang, C. J. Curtis, A. Miedaner, H. M. Pilath and D. L. Dubois, Calculated Hydride Donor Abilities of Five-Coordinate Transition Metal Hydrides [HM(Diphosphine) 2] +(M = Ni, Pd, Pt) as a Function of the Bite Angle and Twist Angle of Diphosphine Ligands, *Organometallics*, 2008, **27**, 2715–2722.
- 18 In addition to the expected dihydride species, in some instances, an additional unidentified species was observed along with the Rh-R-(trans)-Az_b complex (before irradiation) that slowly disappeared upon conversion to the cis configuration with exposure to UV light (Fig. S7†).
- 19 K. Issleib and G. Hohlfeld, Beiträge zur Komplexchemie der Phosphine und Phosphinoxyde. X. Schwermetallkom-

- plexe ditertiärer Phosphine, *Z. Anorg. Allg. Chem.*, 1961, **312** (3–4), 169–179.
- 20 (a) K. Skopek, M. C. Hershberger and J. A. Gladysz, Gyroscopes and the chemical literature: 1852–2002, *Coord. Chem. Rev.*, 2007, **251**(13–14), 1723–1733; (b) K. Skopek, M. C. Hershberger and J. A. Gladysz, Gyroscopes and the chemical literature (1852–2002), *Coord. Chem. Rev.*, 2007, **251**, 1723–1733.
- 21 D. M. Pfund, J. G. Darab, J. L. Fulton and Y. Ma, An XAFS Study of Strontium Ions and Krypton in Supercritical Water, *J. Phys. Chem.*, 1994, **98**(50), 13102–13107.
- 22 J. Stewart, *J. Mol. Model.*, 2007, **13**, 1173–1213.
- 23 J. K. M. Vande Vondele, F. Mohamed, M. Parrinello, T. Chassaing and J. Hutter, *Comput. Phys. Commun.*, 2005, **167**, 103.